Design Strategies and Applications of Nacre – based Biomaterials

Ethan Gerhard[a], Wei Wang[b], Caiyan Li[b], Jinshan Guo[a], Ibrahim Ozbolat[ac], Kevin Rahn[a], April Armstrong[d], Jingfen Xia[b], Guoying Qian[b,*], Jian Yang[a,*]

[a]Department of Biomedical Engineering, Materials Research Institute, The Huck Institutes of the Life Sciences, The Pennsylvania State University, University Park, PA 16802, USA

[b]Zhejiang Provincial Top Key Discipline of Bioengineering, College of Biological and Environmental Sciences, Zhejiang Wanli University, South Qianhu Road 8, Ningbo 315100, China,

[c] Engineering Science and Mechanics Department, Materials Research Institute, The Huck Institutes of the Life Sciences, The Pennsylvania State University, University Park, PA 16802, USA

[d]Department of Orthopaedics and Rehabilitation, College of Medicine, The Pennsylvania State University, Hershey, PA 17033, USA

[*]Corresponding author: Jian Yang, email: jxy30@psu.edu; Guoying Qian, email: qiangy@zwu.edu.cn

Key Words: Biomaterials, nacre, pearl powder, pearl, bone, orthopedic, tissue engineering

Abstract

The field of tissue engineering and regenerative medicine relies heavily on materials capable of implantation without significant foreign body reactions and with the ability to promote tissue differentiation and regeneration. The field of bone tissue engineering in particular requires materials capable of providing enhanced mechanical properties and promoting osteogenic cell lineage commitment. While bone repair has long relied almost exclusively on inorganic, calcium phosphate ceramics such as hydroxyapatite and their composites or on non- degradable metals, the organically derived shell and pearl nacre generated by mollusks has emerged as a promising alternative. Nacre is a naturally occurring composite material composed of inorganic, calcium carbonate plates connected by a framework of organic molecules. Similar to mammalian bone, the highly organized microstructure of nacre endows the composite with superior mechanical properties while the organic phase contributes to significant bioactivity. Studies, both *in vitro*

and *in vivo*, have demonstrated nacre's biocompatibility, biodegradability, and osteogenic potential, which are superior to pure inorganic minerals such as hydroxyapatite or non-degradable metals. Nacre can be used directly as a bulk implant or as part of a composite material when combined with polymers or other ceramics. While nacre has demonstrated its effectiveness in multiple cell culture and animal models, it remains a relatively underexplored biomaterial. This review introduces the formation, structure, and characteristics of nacre, and discusses the present and future uses of this biologically-derived material as a novel biomaterial for orthopedic and other tissue engineering applications.

Introduction

Nacre, commonly known as mother of pearl, is a naturally occurring composite material composed of aragonite (calcium carbonate) platelets cemented by a complex organic matrix. Nacre comprises the inner layer of pearl oyster and freshwater pearl mussel shells as well the pearls themselves, with pearl and shell nacre demonstrating similar chemical compositions as well as high strength, mechanical resilience, and iridescence.

Previous research has demonstrated nacre's biocompatibility, biodegradability, and osteogenic properties, marking nacre's potential as an alternative to other commonly utilized biomaterials in tissue engineering. Nacre has been shown to facilitate osteoblast proliferation and accelerate extracellular matrix (ECM) production and mineralization [1-4]. Additionally, nacre has demonstrated high mechanical strength, excellent biocompatibility, osteogenic capability, and biodegradability both *in vitro* and *in vivo*. The organic matrix contained within nacre has also been found to contain biological molecules capable of activating osteoblasts through chemical signaling; however, research into these organic molecules has been limited [5, 6].

Nacre is a composite consisting of an inorganic mineral phase and an organic matrix, similar to the native structure of bone. This organized structure imparts nacre with its remarkable mechanical strength, while the presence of the organic matrix imparts improved osteoconductivity compared to synthetic materials such as titanium [7]. While orthopedic tissue engineering has previously relied on either autografts or allografts (limited by tissue availability and donor site morbidity) or permanent metal implants, biodegradable materials and composites are the focus of much research in order to provide grafting materials with high availability as well as the potential to be replaced over time by native tissue [8, 9]. Nacre has recently emerged as a potential bone grafting material due to the above-mentioned favorable properties. Bulk nacre as well as composite materials containing nacre as the mineral phase and utilizing various polymers including poly(L-lactic acid) (PLLA), poly(D,L-Lactide) (PDLLA), poly(D,L-Lactide-co-glycolide) (PLGA), ultra-high molecular weight polyethylene (UHMWPE), Polyetheretherketone (PEEK), and poly(3-hydroxybutyrate-co-3-hydroxyvalerate) (PHBV) have been tested as potential biomaterials.

Despite its demonstrated biocompatibility and bioactive properties, to date, no comprehensive review of nacre based materials has been reported and the potential role of nacre based materials in tissue engineering still remains relatively unknown. This paper summarizes current research on nacre, including its basic characteristics as well as its potential use as a biomaterial. Through an examination of relevant literature, the potential of nacre as an alternative to commonly used compositing materials such as hydroxyapatite (HA) and other calcium phosphate minerals for bone tissue engineering will be expounded. Elaboration of the previously conducted research on nacre will demonstrate its potential as a novel and relatively unexplored material for orthopedic

biomaterials science and will stimulate continued research into nacre as an alternative to commonly used biomaterial ceramics such as hydroxyapatite.

Characteristics of Nacre

Formation of Nacre

Nacre is an organized organic-inorganic composite material, secreted by the epithelial cells of the mantle tissue of mollusks. Mantle epithelial cells secrete crystal precursors (Ca^{2+} and CO_3^{2-}) as well as amorphous calcium carbonate, along with organic matrix molecules consisting predominantly of proteins and polysaccharides [10]. In this manner, calcium carbonate forms between the outer layer of mantle epithelial cells and the periosteum membrane. The organic matrix is co-deposited along with the mineral phase, and serves as a critical mineralization regulator.

In nacre, sheets of beta-chitin are interspersed by a hydrophobic gel, containing acidic, aspartic acid rich proteins, forming a highly structured chitinous framework [11]. Amorphous calcium carbonate is deposited at crystal nucleation sites, where it acts as seed molecules for the growth of the aragonite plates that make up the mineral phase of nacre [12]. The process of nacre formation can be summarized as: (1) the formation of a layer of elongated calcite prisms, arranged tightly in a perpendicular orientation to the direction of shell growth, followed by (2) the crystallization of calcium carbonate within the platelets, converting amorphous calcite to a layer of flat, crystalline aragonite platelets [11]. This process is conserved among many species of mollusk (see Table 1).

Pearl formation, when occurring naturally as opposed to artificial seeding, is characterized as a host immune response to intrusion of a foreign body. Typically, a foreign particle or parasite enters the mollusk, prompting local irritation of the mantle tissue and subsequent formation of a

pearl sac to cover the site. A similar process occurs during the pearl forming process when a seed is implanted in the mantle tissue of the mollusk to stimulate the above foreign body response and generate a pearl. Once a pearl sac is formed, nacre is secreted layer by layer to envelope and isolate the irritant, resulting in formation of a pearl after several years. Nacreous pearls are primarily produced by molluscan bivalves or clams. Of the many other molluscan species, few can produce pearls of interest as gemstones. Pearl producing species include the bailer shell *Melo*, the giant clam, *Tridacna*, various scallop species, pen shell *Pinna*, and the *Haliotis iris* species of abalone. Saltwater pearls can be grown in several species of marine pearl oysters in the family *Pteriidae*. Freshwater pearls grow in several species of freshwater mussels including the families *Unionidae* and *Margaritiferidae*.

Table 1: Mollusk Species Capable of Secreting Nacre

Species		**Ref.**	**Species**		**Ref.**
Bivalvia			**Bivalvia**		
Anodonta cygnea	FM*	[13]	*Pinctada imbricate*	MPM	[14]
Lamprotula tortuosa	FM	[15]	*Pinctada margaritifera*	MPM	[16]
Unio pictorum	FM	[17, 18]	*Pinctada martensii*	MPM	[19, 20]
Chamberlainia hainesiana	FPM*	[21]	*Pinctada maxima*	MPM	[22, 23]
Hyriopsis schlegelii	FPM	[24]	*Pinctada radiata*	MPM	[25]
Hyriopsis cumngii	FPM	[26-28]	*Pinna nobilis*	MPM	[19]
Hyriopsis desowitzi	FPM	[21]	*Pinna rudis*	MPM	[19]
Hyriopsis myersiana	FPM	[21]	*Pteria chinensis*	MPM	[29]
Lamellidens marginalis	FPM	[30]	*Pteria hirundo*	MPM	[31]
Lanceolaria glayana	FPM	[15]	*Pteria penguin*	MPM	[32]
Margaritifera dahurica	FPM	[33]	**Gastropoda**		
Margaritifera	FPM	[34, 35]	*Biomphalaria*	FPM	[36]

dahurinaia			*glabrata*		
Magariitfera laevis	FPM	[33]	*Calliostoma zyzyphinus*	FPM	[13]
Margaritifera margaritifera	FPM	[37]	*Gibbula pennant*	MM	[13]
Margaritifera middendorffi	FPM	[33]	*Gibbula umbilicalis*	MM	[13]
Unio tumidus	FPM	[38]	*Haliotis iris*	MM	
Cristaria plicata	FPM	[39]	*Haliotis laevigata*	MM	[40, 41]
Lamprotula leai	FPM	[42]	*Haliotis rufescens*	MM	[43]
Bathymodiolus azoricus	MM*	[44]	*Monodonta sp. ME*	MM	[13]
Isognomon radiatus	MM	[19]	*Trochus niloticus*	MM	
Malleus albus	MM	[19]	*Turbo marmoratus*	MM	
Nucula sulcate	MM	[13]	**Cephalopoda**		
Pteria avicula	MM	[19]	*Nautilus macromphalus*	MM	[45, 46]
Atrina pectinata	MPM*	[19]	*Nautilus pompiplius*	MM	[47]
Mytilus edulis	MPM	[48]	**Monoplacophorans**		
Pinctada fucata	MPM	[49]	*Veleropilina zografi*	MM	[14]

(*FM, freshwater mollusks; FPM, Freshwater pearl mollusks; MPM, Marine pearl mollusks; MM, marine mollusks)

Structure and Characteristics of Nacre

As a natural composite, nacre is known only to occur in mollusks, and is composed of calcium carbonate crystals enclosed in an organic matrix [50], comprising a highly organized, ‘brick and mortar’ or ‘brick wall’ microstructure [46, 47, 51-53]. Within the ‘brick and mortar’ structure (Figure 1), aragonite tablets and thin sheets of organic matrix are alternatively arranged, with aragonite tablets acting as the stacked ‘bricks’ and the organic macromolecules acting as the ‘mortar’, resulting in the superior mechanical properties of the nacre composite [46, 54-56]. This characteristic microarchitecture imparts a fracture resistance over 3,000 fold higher than bulk, geological aragonite [57].

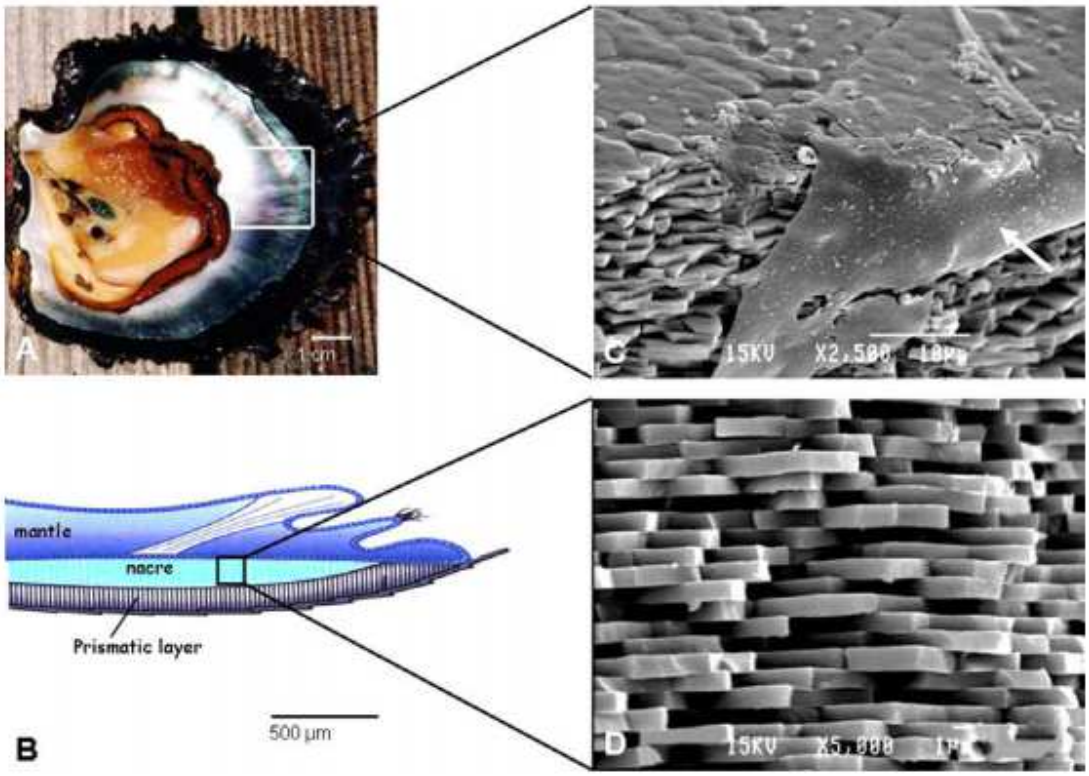

Figure 1: Microstructure of of nacre in P margaritifera. (A) Opened shell displaying internal, iridescent shell nacre layer and brown mantle tissue. (B) Schematic representation of the shell structure and overlying mantle. (C) and (D) The "brick and mortar" structure of the nacreous layer. Reprinted from [46], with permission from Elsevier.

Although nacre is formed in a tightly controlled process, there are several types including columnar and sheet structures. Columnar nacre consists of tablets arranged in a vertical orientation and stacked in columns across the layers and is typically found in *Cephalopoda* and *Gastropoda*. Sheet nacre, in contrast, consists of tablets deposited at the margins of the underlying tablet, resulting in a more random arrangement and is typically found in bivalve species such as oysters and mussels [58].

Nacre is formed from the accumulation of polygonal tablets of aragonite crystal. Typical crystal size ranges from 5 – 15 um in diameter and 0.4 – 0.5 um thick, separated by sheets of interlamellar organic matrices [53, 59-64]. Within the interlamellar organic matrices,

interlamellar sheets are well ordered in a parallel orientation and less than 80 nm from one another [28, 60]. Wang revealed the presence of nanolaths in the nacre tablets about 100 nm in width, with large block twins dividing the nacre tablet into two sectors [52]. Further investigation into the crystallization mechanism of the single crystal nacre tablet could further elucidate the reason and importance of these features.

At the microscale, nanoasperites are present on the surface of the tablets, which have been proposed to act as sources of resistance to tablet sliding. Moreover, the interface between tablets shows a prominent waviness [65]. This waviness contrasts with the previously supposed smooth interface model. The presence of this microstructural motif is thought to be critical to the inelastic deformation and strength of nacre.

Nacreous tablets are stiff and have a high tensile strength, while the interface between tablets has a high compressive stiffness and strength. The hierarchically assembled structure of tablets and matrix endows the composite with its excellent tensile strength and toughness [65, 66]. The mechanical properties of mollusk nacre and shell have been summarized by Heinemann [67]. Due to its structural arrangement, nacre exhibits outstanding mechanical properties: elastic modulus: 64.7 +/- 3.50 GPa, density: 2.6 g/cm^3, and hardness: 4.41 +/- 0.45 GPa [68]. Jackson investigated the mechanical characteristics of nacre from the bivalve *Pincfada*, demonstrating a tensile strength of 140 – 170 MPa, Young's modulus of 60 – 70 GPa, and three point bending value of 350 – 1240 J/m^2 depending on the hydration state [69]. Sarikaya reported wet nacre of the red abalone shell (*H. rufescens*) obtained a fracture toughness of 7 +/- 3 MPa and a strength of 180 +/- 20 MPa while wet nacre of *P. margaritifae* had a fracture toughness of 10 +/- 6 MPa and a strength of 220 +/- 60 MPa [70].

Inspired by the mechanical properties of naturally occurring nacre, much recent research has focused on nacre mimetic materials. Generally, such study has attempted to combine a ceramic component with a relatively elastic, polymeric material. Such combinations offer the distinct advantage of combining the high toughness and damage resistance of ceramic materials with the elasticity and deformability of polymers, resulting in materials with improved fracture resistance, toughness, and mechanical strength. Schmieden created bacteria generated nacre mimetic structures by alternating deposition of $CaCO_3$ by ureolytic bacteria and bacterially produced γ-polyglutamate [71]. Hu utilized liquid crystal self-templating (LCST) to fabricate nacre inspired materials, assembled in a mimetic hierarchy of alternating inorganic nanoplatelets and biomacromolecules. These nacre mimetic composites displayed tensile strengths five to eight times higher than that of natural nacre and excellent ductility (one to two orders of magnitude greater than nacre) [72]. Voet used poly (vinylidene fluoride) lamellae covered with poly (methacrylic acid) as a template to direct silica mineralization, resulting in organized, nacre-like layers [73]. Bai created poly (methyl methacrylate) (PMMA)/ HA composites with nacre mimetic architecture using bidirectional freezing. The obtained materials exhibited moduli of up to 20 GPa, bending strengths up to 100 MPa, and a fracture strength of up to 2075 J/m^2 (~100x monolithic HA) [74]. Hao combined poly (amido amine) and clay nanosheets, cross-linked by genipin, creating biocompatible lamellar composites with a fracture toughness of up to 5103MJ/m^3 [75]. Further modification with $CuSO_4$ resulted in high strength, fluorescent films with antibacterial potential [76]. Sarin generated chitosan/ clay nanoplatelet materials via charge based self-assembly mediated progressive, *in situ* charging of chitosan mediated by hydrolysis of D-glucano-δ-Lactone to D-gluconic acid [77]. Das combined poly (vinyl alcohol) (PVA) and clay nanoplatelets of multiple aspect ratios via concentration induced self-assembly to create a

range of composites with glass-like transparency, excellent gas barrier properties, and varying mechanical properties. Smaller platelets resulted in materials with high toughness while large aspect ratios resulted in stiffer materials (40 GPa) with higher tensile strength (200 MPa) [78]. Mechanical study revealed that smaller plates suffered from pullout failure, while in larger plates, failure by fracture dominated, with the former modality displaying inelastic deformation and the latter toughness and strength similar to cross-linked materials [78].

Graphene has attracted much interest recently as a biomaterial due to its bioactivity, biocompatibility, electrical conductance, and potential for surface modification. As a tailorable nanomaterial, graphene is an ideal candidate for the ceramic phase in nacre mimetic materials. Wan fabricated strong, conductive nacre-like structures using vacuum assisted filtration to align graphene oxide (GO) within a chitosan matrix using the electrostatic interactions between the positively charged chitosan and negatively charged GO under alkaline conditions [79]. Fabricated structures displayed strength 4-10x natural nacre [79]. Lian utilized similar methods to create nacre-like structures from gelatin and ultra large GO, attaining tensile stresses of up to 630.4 MPa through annealing [80]. Duan also achieved high tensile strength and toughness using nanofibrillar cellulose and GO cross-linked with 10,12 pentacosadiyn-1-ol. The impressive mechanical properties were attributed to the breakage of hydrogen bonds followed by the chain stretching of the polymer phase and finally the breakage of covalent bonds, providing a large amount of mechanical dissipation [81]. Chen created paper-like composite films of sodium alginate and GO, with strengths of up to 200 MPa [82]. Li used carboxyl graphene to control the deposition of $CaCO_3$, generating nacre-like morphology with $CaCO_3$ concentration dependent structures [83]. Wan combined GO with molybdenum disulfide nanosheets and thermoplastic polyurethane to form high strength ternary composites with high toughness due to the crack

bridging effect of molybdenum disulfide [84]. Yan generated multifunctional, magnetic, luminescent, and conductive composites combining Fe_3O_4 and lanthanide doped upconversion nanocrystals surface modified with positively charged poly (ethylene imine) and negatively charged GO [85]. Tan successfully fabricated organized structures combining GO and various polymer phases including chitosan, PVA, and poly (ethylene oxide) (PEO), utilizing the attractive forces between charged groups to overcome the repulsion of GO molecules to effect a gel-sol transition and fabricate materials with tensile strengths of up to 200 MPa [86]. Combining ceramics and polymeric phases, nacre-mimetic materials with excellent mechanical properties and multiple functional properties including electrical conductance, fluorescence and optical transparency can be obtained. Given the high degree of modification inherent in this type of assembly as well as the potential of such materials to elucidate composite mechanics, it is expected that future research into nacre-mimetic materials will be robust.

Nacre organic-mineral bonding also displays high thermal stability. Balmain utilized X-ray diffraction to demonstrate two transformations of the aragonite mineral structure when subjected to heating (using acre from the giant oyster, *P maxima*). At 300 – 400 °C, aragonite transforms to calcite, while at 500 – 600°C the calcite transforms to CaO. The organic matrix of nacre displayed high thermal stability, suffering degradation at 550 - 600°C [22]. Due to its high temperature resistance, nacre can polymerize with other materials at high temperatures to attain new composites with improved mechanical characteristics and retained bioactivity.

Several studies have shown that nacre can be transformed into hydroxyapatite, the main inorganic component of vertebrate bone and teeth, via reactions in phosphate buffer solutions. Ni and Ratner found a layer of packed hydroxyapatite particles was formed on the surface of nacre via surface reactions in phosphate buffer at room temperature [87]. These surface reactions

comprise a dissolution – precipitation mechanism in which calcium ions released from the bulk nacre surface enter the phosphate buffer solution and then precipitate as HA on the nacre surface after interacting with free phosphate. X – ray photoelectron spectroscopy (XPS) and secondary ion mass spectroscopy (SIMS) indicated that the mineral phase of the nacre surface had converted from an aragonite phase to an HA phase [73]. Vecchio converted conch and clam shells to HA via a hydrothermal method, demonstrating the formation of dense HA structures on the shell surface at temperatures around 200°C. When treated shells were then implanted in rat femoral defects for 6 weeks, the surfaces of the implants were covered by newly formed bone without evidence of a fibrous tissue layer. These results indicated the biocompatibility and bioactivity of the surface converted nacre [88]. Kobayashi found that large amounts of HA particles could be formed on nacre when heated to 200°C in air followed by soaking in simulated body fluid (SBF). In contrast, when heated to 300°C, above the temperature where destruction of the organic matrix begins, formation of HA particles was retarded, demonstrating the critical role of the organic matrix in HA formation in SBF [89]. Direct conversion of nacre to HA is also observed under high temperature. Lemos discovered a method of converting milled oyster shell into carbonated HA, similar in chemical composition to the carbonated HA found in human bone, via hydrothermal reaction at 200°C [90]. Similarly, Wu converted oyster shell mixed either with calcium pyrophosphate or dicalcium phosphate dihydrate into mixtures of HA and beta-tricalcium phosphate (B-TCP) or pure HA respectively following ball milling and heat treatment [91].

Composition of Nacre

Although composed of more than 95 wt% inorganic aragonite, the organic matrix (5 wt%) is critical not only to the mechanical properties but particularly the bioactivity of nacre [60, 92].

The organic matrix, composed of beta - chitin, silk-like proteins, and acidic glycoproteins rich in aspartic acid, forms the framework between the inorganic mineral phase and has been the subject of extensive research [11, 60]. Almeida found that the amino acid composition of the water soluble matrix (WSM) in *P maxima* is mainly composed of glycine and alanine [93]. Balmain J, using Fourier transform infrared spectroscopy (FT-IR), analyzed the mineral and organic phases of *P maxima*, revealing the presence of amide, amine and carboxyl groups existing at the organic – mineral interface of the nacreous layer. Following decalcification of the sample, the insoluble organic matrix retained amide, amine and carboxyl groups [22]. These studies demonstrated the tight linkage of the matrix proteins and the aragonite phase, which makes separation and purification of the organic components a major challenge. Water extraction is the most widely used, soft extraction method for nacre matrix proteins compared to other methods (acids, resins, EDTA chelation) capable of minimizing loss of molecules; however, this method is still challenging. Therefore, the purification and classification of the WSM remains a challenge and one of the main research goals for nacre.

Bedouet found that the WSM represents approximately 0.24% of the total weight of nacre, with 60% of the WSM made up of low molecular weight molecules (<1kDa), which nevertheless have potential bioactivity [94]. Lamghari suggested that the WSM has functions similar to bone morphogenic protein (BMP) or transforming growth factor – beta (TGF – B), which induce bone growth [95]. Rousseau demonstrated that the WSM had a greater effect on MC3T3-E1 pre-osteoblast cells than dexamethasone, accelerating differentiation and mineralization [3]. Further, the expression of collagen I and the mRNA expression of Runx2 and osteopontin were increased in MC3T3 cells exposed to the low molecular weight WSM. These results indicated the osteogenic potential of the WSM [96]. Milet conducted further testing on several mammalian

cell lines to evaluate the bioactivity of nacre. Bone marrow cells supplemented with WSM began to mineralize following 14 days of culture, and MRC5 fibroblasts displayed an early increase in alkaline phosphatase (ALP) activity [97]. Using 2DE and LC-MS/MS, Oliveiri identified four proteins (three gigasin-2 isoforms and a cystatin A2) for the first time in the WSM of *C gigas* nacre. These proteins are thought to play a part in bone remodeling and biocompatibility [98]. Almeida found that the WSM from *P maxima* could increase ALP activity of cultured human fetal lung tissue fibroblasts [93]. Chaturvedi studied the function of WSM from the nacre of the marine oyster *P fucata,* finding both anti-oxidative and osteogenic differentiation potential [99]. Sud investigated the effects of WSM on mantle cell culture of *P maxima* for 11 days, finding that the WSM reduced the global viability of the cultured cells while increasing ALP activity, which could indicate selective responses to the WSM by different mantle cell types [100]. Chaturvedi investigated the osteoblast differentiation activity of WSM from *P fucata*. The results demonstrated enhanced ALP activity and gene expression of collagen type -1 and osteocalcin [99]. Nacre was also shown to promote wound healing by enhancing cell adhesion and tissue regeneration of skin fibroblasts, stimulating fibroblast mitosis, collagen deposition, and TIMP-1 expression [101].

At the present, many proteins have been successfully purified and identified (Table 2). Bedouet extracted proteinase inhibitors of papain, bovine cathepsin B, and human cathepsin L from the oyster *P margaritifera [102]*. Weiss purified perlucin and perlustrin from the shell of the mollusk *H laevigata* (abalone) by ion-exchange chromatography and reverse-phase HPLC after demineralization of the shell in 10% acetic acid [103]. Yano identified the N19 protein, an important negative regulatory protein in pearl oyster calcification [104]. Yano also identified a protein family of shematrins by cDNA library sequencing in the pearl oyster *P fucata,* which

possessed similar domains comprising repeat sequences of two or more glycines. The results also suggested that shematrins were secreted into the shell and participated in providing a framework for calcification [89]. Fang found a novel protein, PfN23, a key component that regulates the crystal growth in nacre by increasing calcium carbonate deposition and the induction of mineral components into the crystalline, aragonite structure of the mature biocomposite [105].

Although most of the identified proteins were from the soluble part of the organic matrix, they are also constitutive component of the insoluble matrix under certain conditions. Bedouet identified two nacre matrix proteins in the WSM via a proteomics approach; however, one of these proteins was also a critical part of the insoluble matrix [106]. It is thus possible that certain proteins might be transformed from soluble to insoluble under certain conditions in the process of nacre formation.

Other proteins have been discovered unrelated to biomineralization or shell formation. For example, perlucin displays a C-type lectin function and perlustrin shows homology to the N-terminal domain of mammalian insulin-like growth factor (IGF) [40, 107]. Continued research into the protein content of the nacre organic matrix will hopefully reveal the regulatory mechanisms of osteogenesis promoted by nacre.

Table 2: Bioactive Molecules Present in Nacre

Protein	Function	Ref.
AP7	Modulates matrix assembly, nucleation, and crystal growth	[108-111]
AP8	Specifically modifies calcite crystal morphology	[112]
Dermatopontin	Major matrix component, participates in nacre formation	[113]
Lustrin A	Controls calcium carbonate morphology and packing	[114]
MRNP34	Methionine-rich protein associated with biocalcification	[115]

MS17	Important in determining nacre texture	[116, 117]
MS131, MS160	Major components of shell matrix proteins	[118]
N14, N16, pearlin	Exhibits calcium and chitin binding	[119]
n16	Biogenic mineral stabilization	[120]
n16.3	Forms gel-like protein phases to organize single-crystal calcite	[121]
N19	Negative regulatory role in calcification	[104]
N40	Facilitates nucleation of aragonite	[122]
Nautilin-63	Binds chitin, exhibits short collagenous-like domains	[123]
P10	Plays a role in biomineralization	[124]
P43	EDTA-insoluble matrix protein	[125]
P60	Stimulates formation of mineralized nodules	[126]
Perlinhiban	Crystal growth inhibition in nace formation	[127]
Perlucin	Functional C-type lectin	[40]
Perlustrin	Homologue to N-terminal domain of mammalian insulin-like growth factor binding proteins (IGFBPs)	[107]
Perlwapin	Growth inhibitor for calcium carbonate crystals	[128]
PfN23	Key accelerator in control over crystal growth	[105]
PfN44	Stabilizes magnesium calcite to inhibit aragonite deposition	[129]
Pif	Binds to aragonite crystals and regulates nacre formation	[130]
Silkmapin	Shell matrix protein involved in nacre formation	[131]
Upsalin	Mineral associated protein	[132]

Bioactivity of Nacre

Although the organic matrix is quantitatively a minor component of nacre, it is the major active component and controls the formation of nacre [105]. For decades, studies have found that nacre is a bioactive material capable of promoting bone formation *in vitro* and *in vivo*. However, the

mechanism by which nacre stimulates bone differentiation remains largely unknown. It is possible that signal molecules capable of stimulating the osteogenic pathway in mammalian cells reside in nacre [5]. Marin proposed that the organic matrix of nacre was the source of bioactive molecules controlling biomineralization [133]. In addition to its potential as a bone biomaterial, pearl powder and nacre have found applications in beauty products, anti-aging treatments, weight reduction products, and nutritional supplements (via calcium bioavailability) [134-136].

Biocompatibility of Nacre

Nacre and bone are both biomineralized structures, although their composition and organization differ. The mineral phase of human bone is composed of calcium phosphate in the HA crystal form, whereas nacre is composed of calcium carbonate in the aragonite crystal form [87]. Nacre is capable of attracting and activating osteoblasts and is simultaneously biocompatible and osteoinductive, as demonstrated by Silve C [137]. Specifically, perlustrin, an IGF superfamily member found in vertebrates and capable of affecting bone metabolism either by modulating IGF activity or independent of IGF, has been isolated from mollusks and shown to affect osteogenic differentiation [107]. The promising effects of nacre components on mammalian cells with regards to osteogenesis has led to the hypothesis that a similar regulatory mechanism exists in both vertebrates and mollusks. It is possible that the processes of nacre and bone formation, particularly in terms of biomineralization of a calcium based inorganic matrix within an underlying organic framework, are both derived from a common pathway existing during the earliest stages of life, when most, if not all organisms were ocean-bound. It has thus been suggested that nacre and bone have been inherited from a common biomineralization system [6]. This hypothesis has led to the use of nacre as a bone substitute material.

For bone implants, bone bonding is a key factor, and is important for optimal repair. Adhesive surface coatings are required to provide sites for cell anchoring on metal or ceramic implants; however, nacre is capable forming direct bonding with cells. This bonding is facilitated between nacre and newly formed bone via an interlocking calcium and phosphorous front that forms on the nacre surface, resulting from a combination of cell mediated deposition of new mineral as well as conversion of the nacre surface via dissolution – precipitation reactions similar to those observed *in vitro* [138]. Zeta potential measurements of the interfacial structure at the bone – nacre interface have been used to analyze the structure of the region. Results showed that the primary role of the organic matrix proteins was biocompatibility with bone [139]. Atlan placed nacre within the epiphysis of sheep and after 10 months observed direct binding of the bone to the nacre implant [138]. The cells of the osteoprogenitor layer appeared to be contacting the implant surface directly without intervening fibrous tissue. Although the reason for this result was unclear, it may be due to the favorable microenvironment around the nacre implant.

Osteogenic Activity of Nacre

The main characteristics of an osteogenic material are osteoconduction and osteoinduction. It is generally believed that nacre contains one or more signal molecules capable of stimulating bone formation, making it a promising bone biomaterial. Lopez placed nacre chips on a layer of human osteoblasts *in vitro*, resulting in formation of a dense osteoid matrix containing foci with mineralized structural features and bone – like structures. In the presence of nacre from the shell of *P maxima*, bone formation was attained in cultured human osteoblasts, further suggesting the material's ability to stimulate bone formation [113]. Green also observed the osteogenic potential of nacre chips of *P maxima*, with cultured human bone marrow derived stem cells displaying greater ALP expression than BMP-2 treated controls [140]. Lamghari also suggested that nacre

has osteogenic activity via *in vitro* and *in vivo* experiments [95, 141, 142]. Chen found that pearl nanocrystallites were capable of improving the osteogenic ability and promoting the osteogenic differentiation of mouse bone cells (MC3T3 -E1) *in vitro*. Asvanund compared the osteogenic effects of nacre and B-TCP on cocultured human bone cells (HBCs) for four weeks. Results indicated that nacre promoted osteogenic activity by enhancing ALP, bone sialoprotein (BSP), and osteocalcin (OC) expression [143]. Shen demonstrated that, compared to shell nacre and HA, pearl could stimulate the proliferation of osteoblasts more rapidly [4].

The mechanism by which nacre stimulates bone differentiation remains largely unknown. Although most experiments show that nacre is osteogenic, there have been some contrary results. To investigate the interaction between nacre and fresh bone marrow, Bahar placed nacre particles inside demineralized bone matrix (DBM) cylinders filled with fresh rat femur marrow. The cylinders were then implanted subcutaneously at the thoracic region for 4 weeks. The results showed that natural nacre had no osteoinductive performance [144]. Fricain implanted nacre disks or powder from *P margaritifera* subcutaneously in rats for 12 weeks; however, results suggested that the nacre was biodegradable and biocompatible but not osteoinductive [145].

Biodegradability of Nacre

Biodegradability of nacre depends on the size, shape, and location of implants and can be limited in bulk nacre. Duplat showed that nacre obtained from *Pinctada* oyster shell was capable of stimulating resorption of the material by differentiated osteoblasts *in vitro*; however, the rate of resorption was consistently lower than that of bone [146]. Berland implanted raw nacre into sheep bone. After nine months post implantation, the results suggested that smooth surfaced nacre undergoes limited biodegradation and becomes microporous [147]. Osteoclast activity on nacre was studied by Duplat. Pure nacre, obtained from *Pinctada* oyster shell, acted as a

substrate for cell culture of osteoclast stem cells and mature osteoclasts. The results indicated that osteoclasts differentiated from precursor cells on the nacre substrate had the ability to resorb the material. However, compared to osteoclast resorption of bone, the process of nacre resorption was proved to be limited [146]. Liao observed that macrophages and multinucleated giant cells appeared on the degrading nacre implants, indicating biodegradation [148]. Biodegradability of raw nacre is limited *in vivo* due to its well-ordered microstructure. While unfavorable for bone regeneration, this characteristic could be useful in designing artificial dental materials [7].

Design and Applications of Nacre-based Biomaterials

Due to its mechanical strength, biocompatibility and bioactivity as well as additional properties including fluorescence ability, nacre can be utilized as a biomaterial in a variety of applications (Figure 2). Major applications include: (1) implantation of nacre blocks directly as a bone substitute or of bulk composite materials containing nacreous powder, (2) direct injection into bone defects or injection within a bone cement, (3) as a coating for implants and drug delivery vehicles, particularly as a coating to improve the biocompatibility of metal implants, either via physical methods such as electrophoresis or via biological methods in which materials are implanted into the mantle of mollusks and act as irritants, prompting their encapsulation in a pearl coating, (4) as osteogenic additives, particularly incorporation of the WSM into existing biomaterials, and (5) within soft materials and as a naturally occurring nanomaterial, fluorescent material, etc. [149]. Although nacre is naturally compact and hard, replacing part of the calcium carbonate content with other, softer materials could result in a more flexible material while maintaining the nanostructure. Additionally, nacre is a natural nanomaterial that can be used in the field of nanotechnology. Amino acid residues within the tablets could be modified to carry drugs, resulting in novel nanocarriers. Unlike HA, nacre also displays natural fluorescence due to

components of the organic phase (such as conchiolin), a minimally explored property which could be utilized for imaging [150, 151].

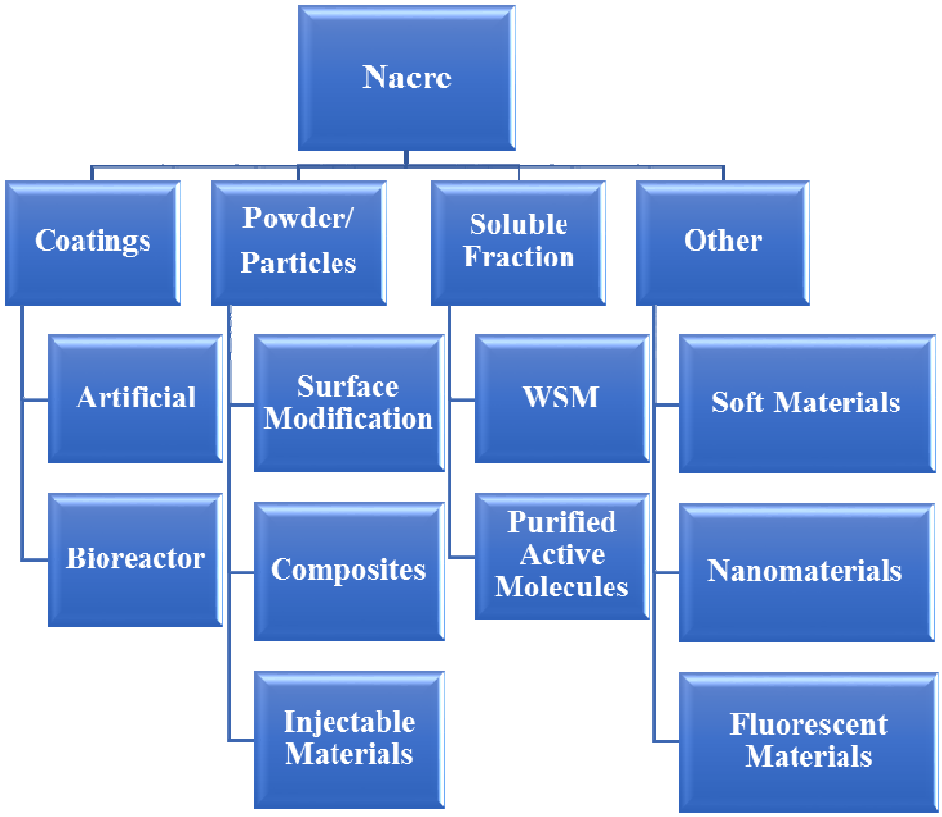

Figure 2: Design strategies and applications of nacre-based biomaterials

Direct Material Implantation

Nacre powder as a bone graft material has been shown to induce new bone formation *in vivo*. Powdered nacre implanted in human jaw bone defects was capable of inducing bone regeneration, with newly formed bone closely contacting the nacre implant [6]. Significant osteoblast activity (Figure 3) was present in the newly formed osteoid border regions, suggesting the osteogenic nature of the nacre implant. Liao implanted nacre granules (<2 mm diameter) into rat femurs, displaying the biocompatibility, biodegradability, and osteoconductivity of nacre. Newly formed bone was formed directly on the nacre surface, with a closely fused interface consisting of a phosphorous rich zone [152]. Lamghari mixed nacre powder (50 - 150 um) with

autologous blood which was injected between the fifth and sixth lumbar vertebrae in an arthritic rabbit model. After two weeks, nacre was well tolerated by the host tissue and after five weeks endochondral bone formation in the region of the degrading nacre particles was detected [153]. After 11 weeks, solid fusion between transverse processes at the implant site was observed [153].

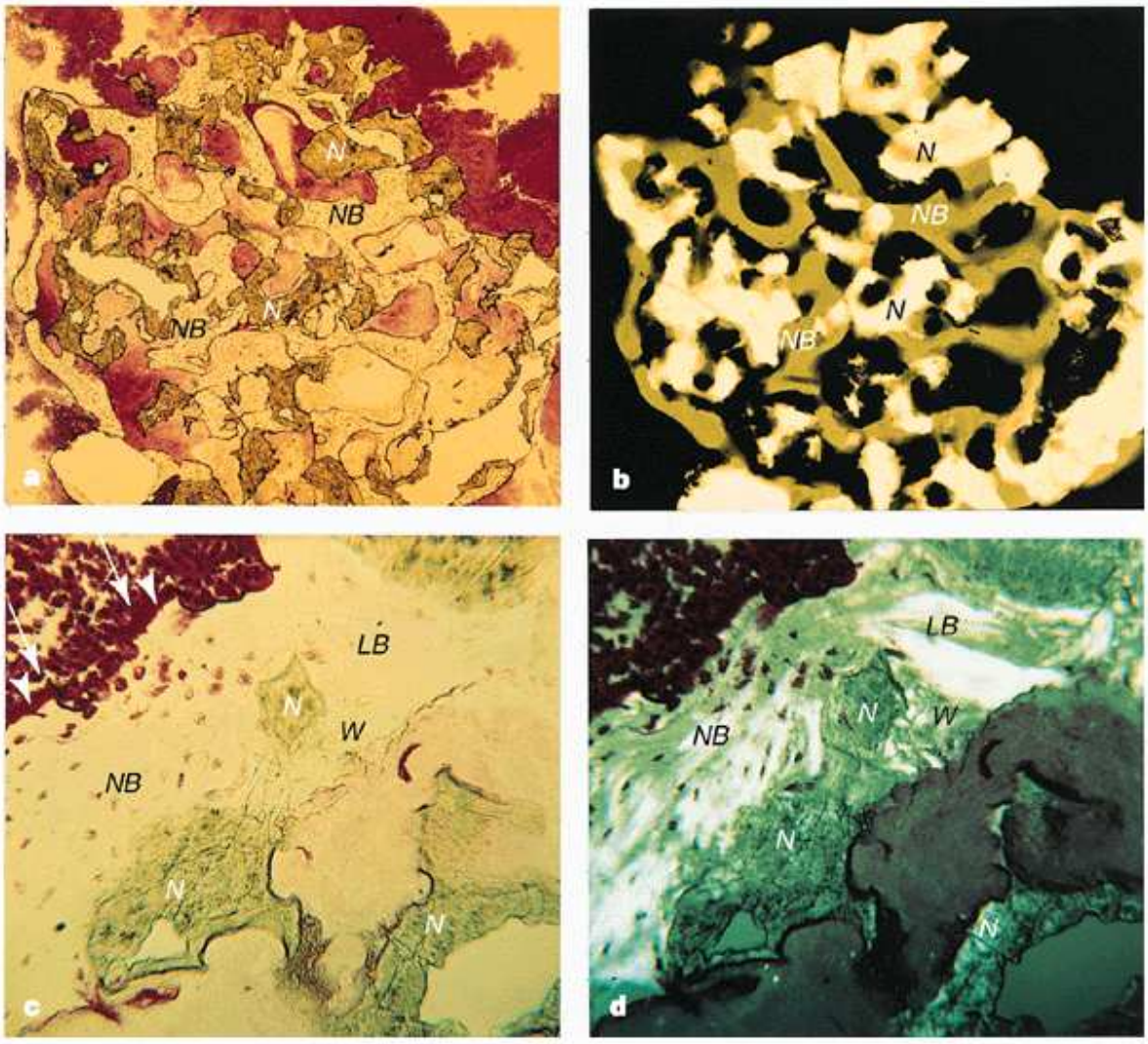

Figure 3: Bone regeneration in defective jawbone following implantation of powdered nacre. (A) and (C) basic fuchsin histological staining, (B) microradiographic imaging, (D) images of decalcified bone biopsy sections, six months after implantation. (C) Arrows indicating osteoblasts in the osteoid border. N, nacre; NB, newly formed bone; W, woven bone; LB, lamellar bone. (A) and (B) 26x magnification; (C) and (D) 157x magnification. Reprinted by permission from Macmillan Publishers Ltd: [6], 1998.

Bulk nacre displays mechanical properties similar to native bone, leading to its use as a bulk grafting material [7]. Nacre plates, screws, and rods were implanted in the first metatarsus of sheep for two months before resection. Results demonstrated the formation of a phosphate rich layer at the bone/ nacre interface, without an interposing fibrous tissue layer. Erosion of the bulk nacre was also observed, forming an irregular surface on which osteoblasts were able to generate new bone. Nacre was thus shown to support a direct interface with bone [138]. Milet placed solid shell nacre within the femur epiphysis of sheep, again demonstrating nacre's ability to support bone tissue generation within an osteoprogenitor rich cell layer [97]. Solid nacre cylinders (6 x 15 mm) were prepared by Atlan and placed within sheep femoral epiphysis. After 10 months, no foreign body response was observed. Moreover, bone formation occurred, with direct binding of newly formed bone with the nacre surface despite minimal degradation of the bulk nacre material [138]. Camprasse tested nacre dental root implants, with excellent union between implanted nacre and human maxillary bone *in vivo* [7]. Liao compared nacre cylinders to Titania/HA composite implants, resulting in an improved bone/ material interface and greater osteogenic activity in the nacre group [9]. Rousseau placed nacre blocks in the subchondral region of the knee in a sheep model to analyze the intra - articular behavior of nacre. New cartilage formation devoid of inflammation was observed after three months [154]. These results demonstrate the potential of nacre as a biomaterial.

Compositing with other Materials

As a raw material, bulk nacre is limited by the difficulty of fabricating desired shapes as well as the slow degradation rate of large implants. Composites composed of nacre and polymeric materials have been developed as an alternative biomaterial for orthopedic tissue regeneration,

displaying enhanced degradation as well as good mechanical, osteoconductive, and osteoinductive properties.

Introducing nacre into PLLA can improve the mechanical properties of the resulting scaffolds. Liu successfully fabricated PLLA/nacre and PLLA/vaterite scaffolds using the freeze drying method. As pearl powder content increased, porosity decreased and yield strength increased [155]. Fabrication of 3D scaffolds of PLLA/aragonite pearl powder, PLLA/vaterite pearl powder, and PLLA/ nacre powder (Figure 4) demonstrated no physical difference among the composites, which attained nearly twice the compressive strength and compressive modulus of pure PLLA. Cell culture with rat bone marrow-derived mesenchymal stem cells (rBMSCs) resulted in increased cell proliferation and ALP activity in the PLLA/ aragonite and PLLA/ nacre groups; however, PLLA/ vaterite displayed the opposite effect [156]. Comparison of the degradation behavior in phosphate buffer solution (PBS) of PLLA, PLLA/ aragonite, and PLLA/vaterite for 200 days demonstrated no difference in degradation rate between the two composites, both of which degraded more slowly than PLLA alone [157]. Dai also fabricated PLA/ nacre powder composites, resulting in an increase in mineralization and cell proliferation versus PLA alone [158].

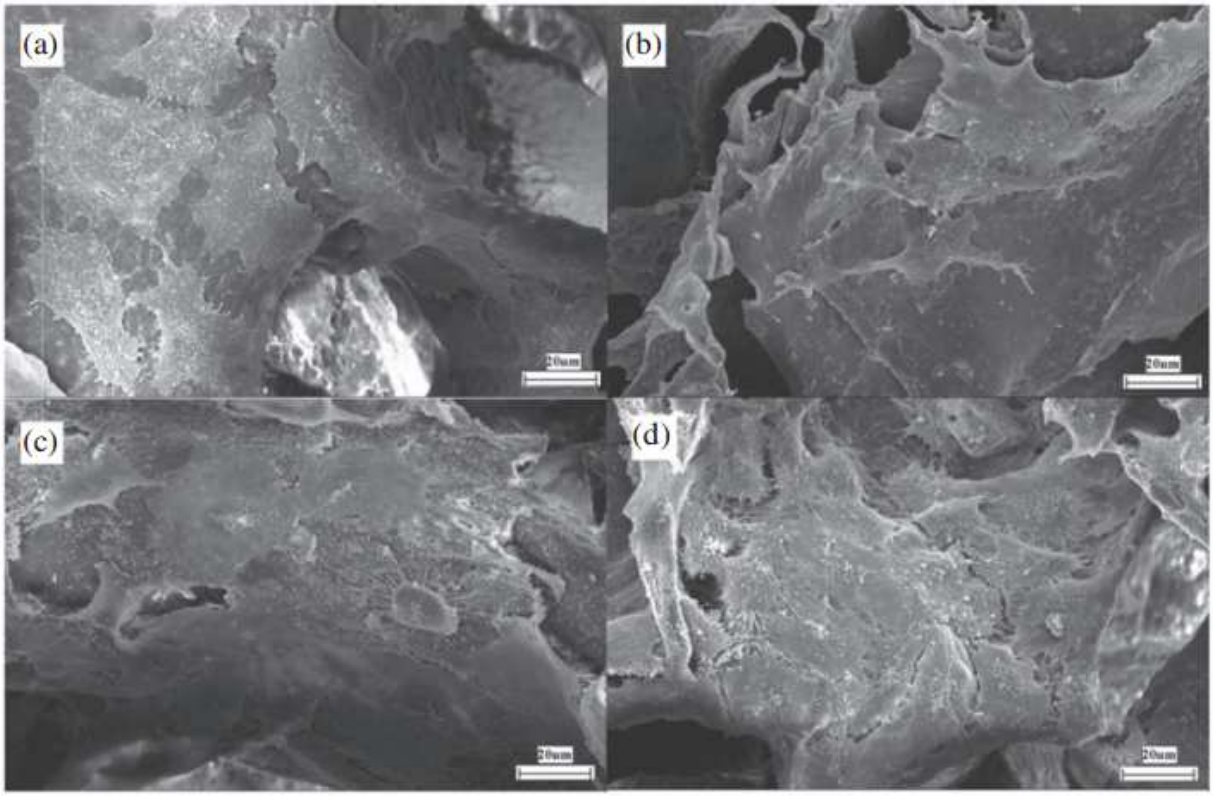

Figure 4: Morphology of rBMSCs on scaffolds 7 days post-seeding. (A) PLLA; (B) PLLA/ vaterite; (C) PLLA/ aragonite; (D) PLLA/ nacre. Reproduced from [135].

A novel, porous PDLLA/ nacre nanocomposite scaffold was fabricated by Xiao. The PDLLA/ nacre scaffold exhibited a high porosity (82.5 +/- 0.8%) and compressive strength in the range of 4.5 +/- 0.25 MPas. *In vitro* and *in vivo* experiments showed that cells adhered and proliferated well on the scaffolds, demonstrating their biocompatibility. The scaffolds were capable of repairing critical size segmental bone defects in rabbits [159].

Yang prepared a hybrid composite scaffold composed of PLGA and nanonized pearl powder. The scaffolds displayed degradation and osteoinduction *in vitro* with MC3T3-E1 cells [160]. Xu developed composite scaffolds of poly(Lactic-co-glycolic acid) (PLGA)/ pearl using low temperature deposition manufacturing (LDM). Resulting scaffolds had high porosity and sufficient pore size and mechanical properties for bone tissue engineering. *In vitro* experiments

indicated that the composites displayed better biocompatibility and osteoconductivity than tricalcium phosphate/ PLGA scaffolds [161].

Liu added ground nacre powder and carbon nanotubes (CNTs) into UHMWPE, coated with perfluoropolyether (PFPE) to fabricate composites. Wear tests demonstrated increased wear resistance for composites versus bulk UHMWPE. Additionally, addition of nacre increased strength versus the bulk polymer [162].

Meifeng fabricated blends of degradable magnesium alloy and pearl powder. Blended alloys were found to alter the corrosion (degradation) rate of the magnesium, creating a more stable implant [163]. Concurrently, inclusion of pearl powder was capable of increasing osteoblast adhesion and proliferation and increasing cytocompatibility [163].

PEEK is a relatively new class of high performance engineering plastic. PEEK has been used to develop implantable joints and ligaments. Tao manufactured pearl powder/ PEEK composite artificial joints composed of a 9:1 ratio of pearl powder: PEEK with a 3 mm thick pearl powder/PEEK layer and a 100 nm pearl powder layer deposited on the bulk implant via a spraying technique. Experimental results showed that the nanometer pearl powder was evenly dispersed and that the composites attained mechanical properties greater than that of titanium composite materials. Cell culture demonstrated a fourfold increase in cell density on pearl powder/ PEEK materials versus pure PEEK [164].

Meng blended pearl powder with PHBV to fabricate films, then treated the films with sodium hydroxide (NaOH) and incubated them in simulated body fluid (SBF) to prepare composite films. Results showed enhanced formation of bone-like apatite. Compositing with pearl powder also improved the films' mechanical properties and hydrophilicity [165]. Bai electrospun PHBV/

pearl powder blends. Compared to neat PHBV, blended fibers displayed improved mineralization and biocompatibility when cultured with MC3T3 cells [166]. Similarly, Deng fabricated electrospun polypropylene/ pearl powder composite monofilaments for pelvic reconstructive mesh, with improved cell proliferation versus polypropylene alone [167].

The above composites have demonstrated the ability of pearl powder and nacre to enhance the mechanical and bioactive properties of bulk polymer materials. However, they require fabrication beforehand and necessitate major surgery for implantation. Therefore, the development of injectable nacreous composites should be considered for *in situ* polymerization, minimizing the trauma of implantation and simplifying manufacturing.

Coating of Materials

Nacreous coatings are advantageous due to the robust mechanical properties, high biocompatibility, and the ability of the nacre interface to promote bone growth. Zhu demonstrated that titanium surface coated with nacre could promote the proliferation and differentiation of MC3T3-E1 cells *in vitro* more effectively than either uncoated or HA coated materials. Cultured cells were larger and had a more spread morphology, possibly due to increased gene expression of transforming growth factor - beta (TGF-beta) 1 [168]. Titanium implants coated with nacre from the fresh water bivalve *H cumingii Lea* cultured with MG-63 cells also promoted the adhesion, proliferation and differentiation of cells [169]. Guo and Zhou fabricated nacre coatings on titanium alloy (Ti6Al4V) via electrophoresis. When subsequently treated in a phosphate solution, the nacre coating was converted via dissolution-precipitation reaction into plate-like apatite with a hierarchical pore structure which showed bioactivity *in vitro* [170]. These promising *in vitro* results should lead to further testing of nacre coatings *in vivo*.

Biofabrication of nacre coatings via direct implantation of materials into the pearl sac of the mollusk has also been studied and is advantageous due to the high mechanical strength of the natural nacre structure deposited on the surface. Coating thickness can be adjusted not only by time but also by implant material choice. Kwan and Wang investigated the biofabrication of nacreous coatings on different materials, indicating the poly(methyl methacrylate) and high density polyethylene were capable of supporting thick coatings (9.8 – 76.5 um) while titanium supported relatively thin coatings (4.4 – 5.9 um) [171]. Wang cultivated titanium dental implants in the pearl sacs of freshwater bivalves, resulting in nacre coatings of approximately 200 - 600 um in thickness after 45 days comprised of a laminated nacreous layer and a transitional, non-laminated layer (Figure 5). Results suggested that nacre coated titanium dental implants could be fabricated via this novel biological technique to form biologically-active and degradable surface coatings [172, 173].

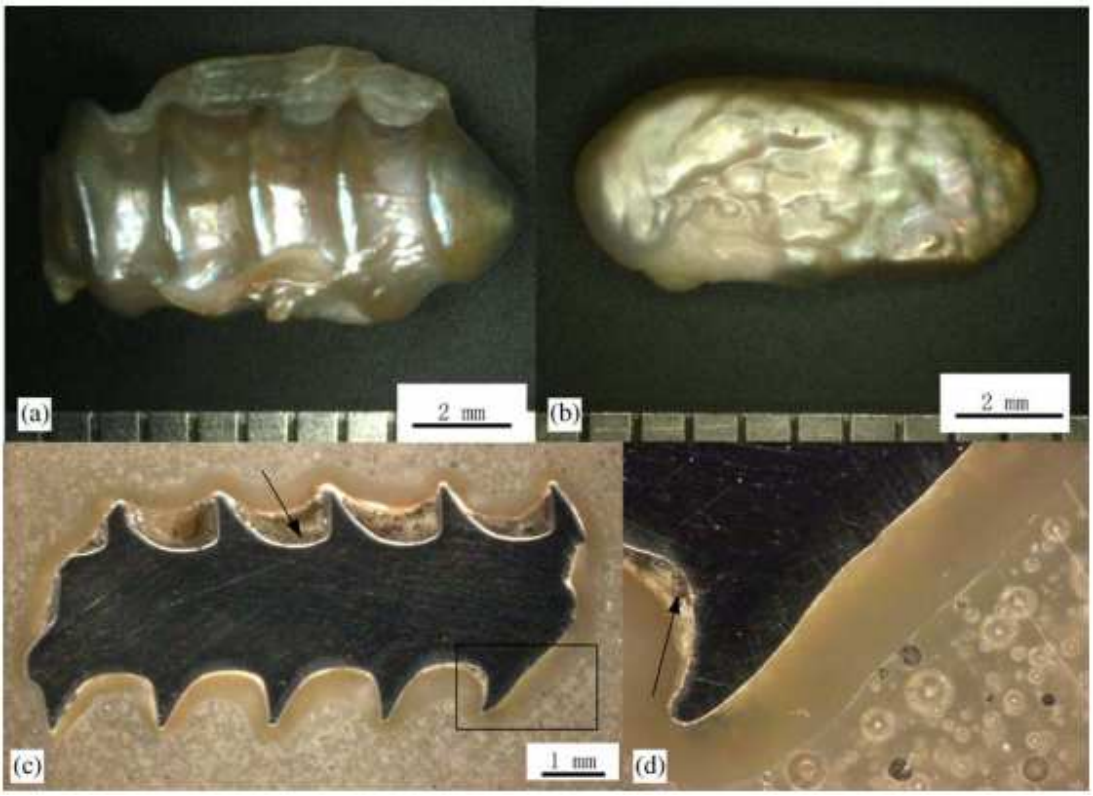

Figure 5: Biological coating of titanium cultured in pearl sacs for 45 days. (A) and (B) Nacreous coatings on dental implant screws and flat plates respectively. (C) Longitudinal section of coated screw. (D) Enlarged image of selected area from (C) showing the interface between the coating and screw. Reprinted from [148], with permission from Elsevier.

Soluble Matrix

Nacre, when implanted *in vivo* in the bones of dogs, sheep, mice, and humans, induces a biological response that includes integration and osteogenic activity that seems to be activated by a set of proteins present in the nacre water soluble matrix (WSM) and ethanol soluble matrix (ESM).

Part of the matrix forming the organic component of nacre is water soluble, and thus may stimulate cells directly in cell culture. Milet investigated the effect of nacre WSM on mammal bone cells, concluding that fibroblasts, human bone marrow stromal cells, and pre - osteoblasts were recruited into an osteogenic pathway, undergoing complete mineralization [97]. Green demonstrated significant increases in proliferation as well as ALP, OCN, and collagen I-IV

expression in bone marrow derived stem cells treated with the WSM of *P maxima* [140]. Using the WSM as a template, Li proposed a new strategy for clinical management of dental caries. WSM was found to be capable of facilitating HA remineralization on eroded human enamel. The highly ordered HA had similar composition and structure to natural enamel, displaying ideal smoothness and hardness [149]. Recently, Brion successfully restored the mineralization capability of subchondral osteoarthritis osteoblasts after 7 days of treatment with the ESM of nacre [174]. Future study will continue to demonstrate the effects of WSM and ESM on cell lineage commitment.

Conclusion

A highly organized organic - inorganic composite material, nacre not only demonstrates excellent mechanical properties due to its complex architecture, but also displays biocompatibility as well as bioactivity that is absent in HA and other ceramic materials commonly used in orthopedic tissue engineering. Nacre as a bulk material, as a coating, or as part of a composite with polymeric materials can be utilized to develop a wide range of biomaterials capable of promoting bone tissue regeneration while remaining degradable. Nacre powder or the WSM can be used as direct injectable materials or part of cements or other self - setting systems. Nacre also has the potential for modification to serve as a drug carrier or to create novel materials demonstrating improved physical properties versus bulk nacre (i.e. accelerated degradation, enhanced elasticity, and improved molding/ processing). Similar to HA and calcium phosphate, nacre can also be utilized in three-dimensional printing as a reinforcement material within hard polymers or soft hydrogels. Although currently relatively unknown compared to HA and calcium phosphates, future research will continue to demonstrate

the superior bioactivity and novel properties of nacre for orthopedic tissue regeneration, leading to a new class of materials and composites based on this biologically derived product.

Acknowledgement

This work was supported in part by National Institutes of Health awards (CA182670, HL118498) and National Science Foundation (NSF) award (CMMI 1537008).

References

[1] Flausse A, Henrionnet C, Dossot M, Dumas D, Hupont S, Pinzano A, Mainard D, Galois L, Magdalou J, Lopez E. Osteogenic differentiation of human bone marrow mesenchymal stem cells in hydrogel containing nacre powder. Journal of Biomedical Materials Research Part A 2013;101:3211-8.
[2] Lopez E, Le Faou A, Borzeix S, Berland S. Stimulation of rat cutaneous fibroblasts and their synthetic activity by implants of powdered nacre (mother of pearl). Tissue and Cell 2000;32:95-101.
[3] Rousseau M, Pereira-Mouriès L, Almeida M-J, Milet C, Lopez E. The water-soluble matrix fraction from the nacre of Pinctada maxima produces earlier mineralization of MC3T3-E1 mouse pre-osteoblasts. Comparative Biochemistry and Physiology Part B: Biochemistry and Molecular Biology 2003;135:1-7.
[4] Shen Y, Zhu J, Zhang H, Zhao F. In vitro osteogenetic activity of pearl. Biomaterials 2006;27:281-7.
[5] Mouriès LP, Almeida M-J, Milet C, Berland S, Lopez E. Bioactivity of nacre water-soluble organic matrix from the bivalve mollusk Pinctada maxima in three mammalian cell types: fibroblasts, bone marrow stromal cells and osteoblasts. Comparative Biochemistry and Physiology Part B: Biochemistry and Molecular Biology 2002;132:217-29.
[6] Westbroek P, Marin F. A marriage of bone and nacre. Nature 1998;392:861-2.
[7] Camprasse S, Camprasse G, Pouzol M, Lopez E. Artificial dental root made of natural calcium carbonate (Bioracine). Clinical materials 1990;5:235-50.
[8] Delattre O, Catonne Y, Berland S, Borzeix S, Lopez E. Use of mother of pearl as a bone substitute-Experimental study in sheep. European Journal of Orthopaedic Surgery & Traumatology 1997;7:143-7.
[9] Liao H, Brandsten C, Lundmark C, Wurtz T, Li J. Responses of bone to titania–hydroxyapatite composite and nacreous implants: a preliminary comparison by in situ hybridization. Journal of Materials Science: Materials in Medicine 1997;8:823-7.
[10] Addadi L, Joester D, Nudelman F, Weiner S. Mollusk shell formation: a source of new concepts for understanding biomineralization processes. Chemistry–A European Journal 2006;12:980-7.
[11] Kröger N. The molecular basis of nacre formation. Science 2009;325:1351-2.

[12] Nudelman F, Chen HH, Goldberg HA, Weiner S, Addadi L. Spiers Memorial Lecture Lessons from biomineralization: comparing the growth strategies of mollusc shell prismatic and nacreous layers in Atrina rigida. Faraday discussions 2007;136:9-25.
[13] Checa AG, Cartwright JH, Willinger M-G. Mineral bridges in nacre. Journal of structural biology 2011;176:330-9.
[14] Checa AG, Ramírez-Rico J, González-Segura A, Sánchez-Navas A. Nacre and false nacre (foliated aragonite) in extant monoplacophorans (= Tryblidiida: Mollusca). Naturwissenschaften 2009;96:111-22.
[15] Wang G, Cao X, Li J. Complete F-type mitochondrial genome of Chinese freshwater mussel Lamprotula tortuosa. Mitochondrial DNA 2013;24:513-5.
[16] Dauphin Y, Ball AD, Cotte M, Cuif J-P, Meibom A, Salomé M, Susini J, Williams CT. Structure and composition of the nacre–prisms transition in the shell of Pinctada margaritifera (Mollusca, Bivalvia). Analytical and Bioanalytical Chemistry 2008;390:1659-69.
[17] Marie B, Luquet G, Bédouet L, Milet C, Guichard N, Medakovic D, Marin F. Nacre calcification in the freshwater mussel Unio pictorum: carbonic anhydrase activity and purification of a 95 kDa calcium-binding glycoprotein. ChemBioChem 2008;9:2515-23.
[18] Marie B, Luquet G, Pais De Barros JP, Guichard N, Morel S, Alcaraz G, Bollache L, Marin F. The shell matrix of the freshwater mussel Unio pictorum (Paleoheterodonta, Unionoida). Febs Journal 2007;274:2933-45.
[19] Checa AG, Rodríguez-Navarro AB. Self-organisation of nacre in the shells of Pterioida (Bivalvia: Mollusca). Biomaterials 2005;26:1071-9.
[20] Jiao Y, Wang H, Du X, Zhao X, Wang Q, Huang R, Deng Y. Dermatopontin, a shell matrix protein gene from pearl oyster Pinctada martensii, participates in nacre formation. Biochemical and biophysical research communications 2012;425:679-83.
[21] Vannarattanarat S, Zieritz A, Kanchanaketu T, Kovitvadhi U, Kovitvadhi S, Hongtrakul V. Molecular identification of the economically important freshwater mussels (Mollusca–Bivalvia–Unionoida) of Thailand: developing species-specific markers from AFLPs. Animal genetics 2014;45:235-9.
[22] Balmain J, Hannoyer B, Lopez E. Fourier transform infrared spectroscopy (FTIR) and X-ray diffraction analyses of mineral and organic matrix during heating of mother of pearl (nacre) from the shell of the mollusc Pinctada maxima. Journal of biomedical materials research 1999;48:749-54.
[23] Zentz F, Bédouet L, Almeida MJ, Milet C, Lopez E, Giraud M. Characterization and quantification of chitosan extracted from nacre of the abalone Haliotis tuberculata and the oyster Pinctada maxima. Marine Biotechnology 2001;3:36-44.
[24] He S, Peng K, Hong Y, Wang J, Sheng J, Gu Q. Molecular properties and immune defense of two ferritin subunits from freshwater pearl mussel, Hyriopsis schlegelii. Fish & shellfish immunology 2013;34:865-74.
[25] Pourang N, Richardson C, Chenery S, Nasrollahzedeh H. Assessment of trace elements in the shell layers and soft tissues of the pearl oyster Pinctada radiata using multivariate analyses: a potential proxy for temporal and spatial variations of trace elements. Environmental monitoring and assessment 2014;186:2465-85.
[26] Bai Z, Zheng H, Lin J, Wang G, Li J. Comparative analysis of the transcriptome in tissues secreting purple and white nacre in the pearl mussel Hyriopsis cumingii. PloS one 2013;8:e53617.

[27] Tao J, Xu Y-z, Weng S-f, Wu J-g, Xu D-f. [FTIR study on structure of pearl and nacre of mollusk shell]. Guang pu xue yu guang pu fen xi= Guang pu 1998;18:307-10.
[28] Xie L, Wang X-X, Li J. The SEM and TEM study on the laminated structure of individual aragonitic nacre tablet in freshwater bivalve H. cumingii Lea shell. Journal of structural Biology 2010;169:89-94.
[29] Guenther J, De Nys R. Differential community development of fouling species on the pearl oysters Pinctada fucata, Pteria penguin and Pteria chinensis (Bivalvia, Pteriidae). Biofouling 2006;22:151-9.
[30] Chakraborty M, Bhattacharya S, Mishra R, Mukherjee D, Mishra R. Antioxidant content and activity of the Indian fresh-water pearl mussel in the prevention of arthritis in an experimental animal model. British Journal of Nutrition 2012;108:1346-50.
[31] Osuna-Mascaró AJ, Cruz-Bustos T, Marin F, Checa AG. Ultrastructure of the Interlamellar Membranes of the Nacre of the Bivalve Pteria hirundo, Determined by Immunolabelling. PloS one 2015;10:e0122934.
[32] Naganuma T, Hoshino W, Shikanai Y, Sato R, Liu K, Sato S, Muramoto K, Osada M, Yoshimi K, Ogawa T. Novel matrix proteins of Pteria penguin pearl oyster shell nacre homologous to the jacalin-related β-prism fold lectins. PloS one 2014;9:e112326.
[33] Bolotov IN, Bespalaya YV, Vikhrev IV, Aksenova OV, Aspholm PE, Gofarov MY, Klishko OK, Kolosova YS, Kondakov AV, Lyubas AA. Taxonomy and Distribution of Freshwater Pearl Mussels (Unionoida: Margaritiferidae) of the Russian Far East. PloS one 2015;10:e0122408.
[34] Bogatov V. Pearl Mussels (Bivalvia, Margaritiferidae, Dahurinaia) from the Amur River Basin. Biology Bulletin 2012;39:672-5.
[35] Klishko O. Pearl mussels of the genus Dahurinaia (Bivalvia, Margaritiferidae): Differently sized groups of Margaritifera dahurica Middendorff, 1850. Biology Bulletin 2014;41:434-43.
[36] Richards CS. Biomphalaria glabrata genetics: Pearl formation. Journal of invertebrate pathology 1972;20:37-40.
[37] Ziuganov V. [Arctic and southern freshwater pearl mussel Margaritifera margaritifera with long and short life span as a model system for testing longevity mechanisms]. Advances in gerontology= Uspekhi gerontologii/Rossiiskaia akademiia nauk, Gerontologicheskoe obshchestvo 2003;14:21-30.
[38] Ginzburg E, Mashanskiĭ V. [Action of increased temperature on the lateral cells of the ciliated epithelium of the gills of the pearl oyster (Unio tumidus). II. Change in the ultrastructure of the cytoplasm]. Tsitologiia 1973;15:1085-90.
[39] Lee JH, Choi EH, Kim SK, Ryu SH, Hwang UW. Mitochondrial genome of the cockscomb pearl mussel Cristaria plicata (Bivalvia, Unionoida, Unionidae). Mitochondrial DNA 2012;23:39-41.
[40] Mann K, Weiss IM, André S, Gabius HJ, Fritz M. The amino-acid sequence of the abalone (Haliotis laevigata) nacre protein perlucin. European Journal of Biochemistry 2000;267:5257-64.
[41] Nassif N, Pinna N, Gehrke N, Antonietti M, Jäger C, Cölfen H. Amorphous layer around aragonite platelets in nacre. Proceedings of the National Academy of Sciences of the United States of America 2005;102:12653-5.
[42] Jin-Jin M, Rong-Hui Y, Gen-Fang ZHANG R-QZ. Microsatellite analysis of genetic diversity and population structure of freshwater mussel (Lamprotula leai). Zoological Research 2015;36:34.

[43] Gilbert P, Metzler RA, Zhou D, Scholl A, Doran A, Young A, Kunz M, Tamura N, Coppersmith SN. Gradual ordering in red abalone nacre. Journal of the American Chemical Society 2008;130:17519-27.
[44] Kadar E, Checa AG, Oliveira AN, Machado JP. Shell nacre ultrastructure and depressurisation dissolution in the deep-sea hydrothermal vent mussel Bathymodiolus azoricus. Journal of Comparative Physiology B 2008;178:123-30.
[45] Marie B, Marin F, Marie A, Bédouet L, Dubost L, Alcaraz G, Milet C, Luquet G. Evolution of nacre: biochemistry and proteomics of the shell organic matrix of the cephalopod Nautilus macromphalus. ChemBioChem 2009;10:1495-506.
[46] Rousseau M, Meibom A, Gèze M, Bourrat X, Angellier M, Lopez E. Dynamics of sheet nacre formation in bivalves. Journal of structural biology 2009;165:190-5.
[47] Bezares J, Asaro RJ, Hawley M. Macromolecular structure of the organic framework of nacre in Haliotis rufescens: implications for growth and mechanical behavior. Journal of structural biology 2008;163:61-75.
[48] Zuykov M, Pelletier E, Belzile C, Demers S. Alteration of shell nacre micromorphology in blue mussel Mytilus edulis after exposure to free-ionic silver and silver nanoparticles. Chemosphere 2011;84:701-6.
[49] Li S, Xie L, Zhang C, Zhang Y, Gu M, Zhang R. Cloning and expression of a pivotal calcium metabolism regulator: calmodulin involved in shell formation from pearl oyster (Pinctada fucata). Comparative Biochemistry and Physiology Part B: Biochemistry and Molecular Biology 2004;138:235-43.
[50] Weiner S, Hood L. Soluble protein of the organic matrix of mollusk shells: a potential template for shell formation. Science 1975;190:987-9.
[51] Bezares J, Asaro RJ, Hawley M. Macromolecular structure of the organic framework of nacre in Haliotis rufescens: implications for mechanical response. Journal of structural biology 2010;170:484-500.
[52] Wang S-N, Yan X-H, Wang R, Yu D-H, Wang X-X. A microstructural study of individual nacre tablet of Pinctada maxima. Journal of structural biology 2013;183:404-11.
[53] Watabe N. Studies on shell formation: XI. Crystal—matrix relationships in the inner layers of mollusk shells. Journal of ultrastructure research 1965;12:351-70.
[54] Currey JD, Zioupos P, Peter D, Casinos A. Mechanical properties of nacre and highly mineralized bone. Proceedings of the Royal Society of London B: Biological Sciences 2001;268:107-11.
[55] Sumitomo T, Kakisawa H, Kagawa Y. Nanoscale structure and mechanical behavior of growth lines in shell of abalone Haliotis gigantea. Journal of structural biology 2011;174:31-6.
[56] Wise SW. Microarchitecture and deposition of gastropod nacre. Science 1970;167:1486-8.
[57] Dashkovskiy S, Suhr B, Tushtev K, Grathwohl G. Nacre properties in the elastic range: Influence of matrix incompressibility. Computational Materials Science 2007;41:96-106.
[58] Dauphin Y. Structure and composition of the septal nacreous layer of Nautilus macromphalus L.(Mollusca, Cephalopoda). Zoology 2006;109:85-95.
[59] Grégoire C. Topography of the organic components in mother-of-pearl. The Journal of biophysical and biochemical cytology 1957;3:797-808.
[60] Levi-Kalisman Y, Falini G, Addadi L, Weiner S. Structure of the nacreous organic matrix of a bivalve mollusk shell examined in the hydrated state using cryo-TEM. Journal of structural biology 2001;135:8-17.

[61] Reimann BEF, Lewin JC, Volcani B. Studies on the biochemistry and fine structure of silica shell formation in diatoms I. The structure of the cell wall of Cylindrotheca fusiformis Reimann and Lewin. The Journal of cell biology 1965;24:39-55.
[62] Rousseau M, Lopez E, Couté A, Mascarel G, Smith DC, Naslain R, Bourrat X. Sheet nacre growth mechanism: a Voronoi model. Journal of structural biology 2005;149:149-57.
[63] Takahashi K, Yamamoto H, Onoda A, Doi M, Inaba T, Chiba M, Kobayashi A, Taguchi T, Okamura T-a, Ueyama N. Highly oriented aragonite nanocrystal–biopolymer composites in an aragonite brick of the nacreous layer of Pinctada fucata. Chemical Communications 2004:996-7.
[64] Xu L-P, Peng J, Liu Y, Wen Y, Zhang X, Jiang L, Wang S. Nacre-inspired design of mechanical stable coating with underwater superoleophobicity. ACS nano 2013;7:5077-83.
[65] Barthelat F, Tang H, Zavattieri P, Li C-M, Espinosa H. On the mechanics of mother-of-pearl: a key feature in the material hierarchical structure. Journal of the Mechanics and Physics of Solids 2007;55:306-37.
[66] Shao Y, Zhao H-P, Feng X-Q. On flaw tolerance of nacre: a theoretical study. Journal of The Royal Society Interface 2014;11:20131016.
[67] Heinemann F, Launspach M, Gries K, Fritz M. Gastropod nacre: structure, properties and growth—biological, chemical and physical basics. Biophysical chemistry 2011;153:126-53.
[68] Denkena B, Koehler J, Moral A. Ductile and brittle material removal mechanisms in natural nacre—A model for novel implant materials. Journal of Materials Processing Technology 2010;210:1827-37.
[69] Jackson A, Vincent J, Turner R. The mechanical design of nacre. Proceedings of the Royal Society of London B: Biological Sciences 1988;234:415-40.
[70] Sarikaya M, Aksay IA. Nacre of abalone shell: a natural multifunctional nanolaminated ceramic-polymer composite material. Structure, cellular synthesis and assembly of biopolymers: Springer; 1992. p. 1-26.
[71] Schmieden DT, Meyer AS, Aubin-Tam M-E. Using bacteria to make improved, nacre-inspired materials. MRS Advances 2016;1:559-64.
[72] Hu X, Xu Z, Liu Z, Gao C. Liquid crystal self-templating approach to ultrastrong and tough biomimic composites. Scientific reports 2013;3.
[73] Voet VS, Kumar K, Brinke Gt, Loos K. Bioinspired Synthesis of Well-Ordered Layered Organic–Inorganic Nanohybrids: Mimicking the Natural Processing of Nacre by Mineralization of Block Copolymer Templates. Macromolecular Rapid Communications 2015;36:1756-60.
[74] Bai H, Walsh F, Gludovatz B, Delattre B, Huang C, Chen Y, Tomsia AP, Ritchie RO. Bioinspired Hydroxyapatite/Poly (methyl methacrylate) Composite with a Nacre-Mimetic Architecture by a Bidirectional Freezing Method. Advanced Materials 2016;28:50-6.
[75] Hao W, Zhang L, Wang X, Wang J, Hu Z, Yang W. Tough and strong nacre-like composites from hyperbranched poly(amido amine) and clay nanosheets cross-linked by genipin. RSC Advances 2016;6:1415-21.
[76] Hao W, Wang X, Ding S, Cao Y, Zhang H, Yang W. Robust, antibacterial, and fluorescent hybrid films mimicking nacre. RSC Advances 2015;5:86861-6.
[77] Sarin S, Kolesnikova S, Postnova I, Ha C-S, Shchipunov Y. Bionanocomposite from self-assembled building blocks of nacre-like crystalline polymorph of chitosan with clay nanoplatelets. RSC Advances 2016;6:33501-9.
[78] Das P, Malho J-M, Rahimi K, Schacher FH, Wang B, Demco DE, Walther A. Nacre-mimetics with synthetic nanoclays up to ultrahigh aspect ratios. Nature communications 2015;6.

[79] Wan S, Peng J, Li Y, Hu H, Jiang L, Cheng Q. Use of synergistic interactions to fabricate strong, tough, and conductive artificial nacre based on graphene oxide and chitosan. ACS nano 2015;9:9830-6.
[80] Lian M, Fan J, Shi Z, Zhang S, Li H, Yin J. Gelatin-assisted fabrication of graphene-based nacre with high strength, toughness, and electrical conductivity. Carbon 2015;89:279-89.
[81] Duan J, Gong S, Gao Y, Xie X, Jiang L, Cheng Q. Bioinspired Ternary Artificial Nacre Nanocomposites Based on Reduced Graphene Oxide and Nanofibrillar Cellulose. ACS applied materials & interfaces 2016;8:10545-50.
[82] Chen K, Shi B, Yue Y, Qi J, Guo L. Binary synergy strengthening and toughening of bio-inspired nacre-like graphene oxide/sodium alginate composite paper. ACS nano 2015;9:8165-75.
[83] Li J, Liu D, Li B, Wang J, Han S, Liu L, Wei H. A bio-inspired nacre-like layered hybrid structure of calcium carbonate under the control of carboxyl graphene. CrystEngComm 2015;17:520-5.
[84] Wan S, Li Y, Peng J, Hu H, Cheng Q, Jiang L. Synergistic Toughening of Graphene Oxide–Molybdenum Disulfide–Thermoplastic Polyurethane Ternary Artificial Nacre. ACS nano 2015;9:708-14.
[85] Yan L, Chang YN, Yin W, Tian G, Zhou L, Hu Z, Xing G, Gu Z, Zhao Y. Enhanced Multifunctional Properties of Graphene Nanocomposites with Nacre-Like Structures. Advanced Engineering Materials 2015;17:523-31.
[86] Tan Z, Zhang M, Li C, Yu S, Shi G. A General Route to Robust Nacre-Like Graphene Oxide Films. ACS applied materials & interfaces 2015;7:15010-6.
[87] Ni M, Ratner BD. Nacre surface transformation to hydroxyapatite in a phosphate buffer solution. Biomaterials 2003;24:4323-31.
[88] Vecchio KS, Zhang X, Massie JB, Wang M, Kim CW. Conversion of bulk seashells to biocompatible hydroxyapatite for bone implants. Acta biomaterialia 2007;3:910-8.
[89] Kobayashi S, Ui M, Araikawa H, Sakamoto T, Nakai K. Effect of Heat Treatments of Bioactive Nacre on HAp Formation in SBF. Materials Science Forum: Trans Tech Publ; 2012. p. 526-31.
[90] Lemos A, Rocha J, Quaresma S, Kannan S, Oktar F, Agathopoulos S, Ferreira J. Hydroxyapatite nano-powders produced hydrothermally from nacreous material. Journal of the European Ceramic Society 2006;26:3639-46.
[91] Wu S-C, Hsu H-C, Wu Y-N, Ho W-F. Hydroxyapatite synthesized from oyster shell powders by ball milling and heat treatment. Materials characterization 2011;62:1180-7.
[92] Barthelat F, Espinosa H. An experimental investigation of deformation and fracture of nacre–mother of pearl. Experimental mechanics 2007;47:311-24.
[93] Almeida MJ, Milet C, Peduzzi J, Pereira L, Haigle J, Barthélemy M, Lopez E. Effect of water-soluble matrix fraction extracted from the nacre of Pinctada maxima on the alkaline phosphatase activity of cultured fibroblasts. Journal of Experimental Zoology 2000;288:327-34.
[94] Bédouet L, Rusconi F, Rousseau M, Duplat D, Marie A, Dubost L, Le Ny K, Berland S, Péduzzi J, Lopez E. Identification of low molecular weight molecules as new components of the nacre organic matrix. Comparative Biochemistry and Physiology Part B: Biochemistry and Molecular Biology 2006;144:532-43.
[95] Lamghari M, Almeida M, Berland S, Huet H, Laurent A, Milet C, Lopez E. Stimulation of bone marrow cells and bone formation by nacre: in vivo and in vitro studies. Bone 1999;25:91S-4S.

[96] Rousseau M, Boulzaguet H, Biagianti J, Duplat D, Milet C, Lopez E, Bédouet L. Low molecular weight molecules of oyster nacre induce mineralization of the MC3T3-E1 cells. Journal of Biomedical Materials Research Part A 2008;85:487-97.
[97] Milet C, Berland S, Lamghari M, Mouries L, Jolly C, Borzeix S, Doumenc D, Lopez É. Conservation of signal molecules involved in biomineralisation control in calcifying matrices of bone and shell. Comptes Rendus Palevol 2004;3:493-501.
[98] Oliveira DV, Silva TS, Cordeiro OD, Cavaco SI, Simes DC. Identification of proteins with potential osteogenic activity present in the water-soluble matrix proteins from Crassostrea gigas nacre using a proteomic approach. The Scientific World Journal 2012;2012.
[99] Chaturvedi R, Singha PK, Dey S. Water soluble bioactives of nacre mediate antioxidant activity and osteoblast differentiation. PloS one 2013;8:e84584.
[100] Sud D, Doumenc D, Lopez E, Milet C. Role of water-soluble matrix fraction, extracted from the nacre of Pinctada maxima, in the regulation of cell activity in abalone mantle cell culture (Haliotis tuberculata). Tissue and Cell 2001;33:154-60.
[101] Li Y-C, Chen C-R, Young T-H. Pearl extract enhances the migratory ability of fibroblasts in a wound healing model. Pharmaceutical biology 2013;51:289-97.
[102] Bédouet L, Duplat D, Marie A, Dubost L, Berland S, Rousseau M, Milet C, Lopez E. Heterogeneity of proteinase inhibitors in the water-soluble organic matrix from the oyster nacre. Marine biotechnology 2007;9:437-49.
[103] Weiss IM, Kaufmann S, Mann K, Fritz M. Purification and characterization of perlucin and perlustrin, two new proteins from the shell of the mollusc Haliotis laevigata. Biochemical and biophysical research communications 2000;267:17-21.
[104] Yano M, Nagai K, Morimoto K, Miyamoto H. A novel nacre protein N19 in the pearl oyster Pinctada fucata. Biochemical and biophysical research communications 2007;362:158-63.
[105] Fang D, Pan C, Lin H, Lin Y, Zhang G, Wang H, He M, Xie L, Zhang R. Novel basic protein, PfN23, functions as key macromolecule during nacre formation. Journal of Biological Chemistry 2012;287:15776-85.
[106] Bédouet L, Marie A, Dubost L, Péduzzi J, Duplat D, Berland S, Puisségur M, Boulzaguet H, Rousseau M, Milet C. Proteomics analysis of the nacre soluble and insoluble proteins from the oyster Pinctada margaritifera. Marine Biotechnology 2007;9:638-49.
[107] Weiss IM, Göhring W, Fritz M, Mann K. Perlustrin, a Haliotis laevigata (abalone) nacre protein, is homologous to the insulin-like growth factor binding protein N-terminal module of vertebrates. Biochemical and biophysical research communications 2001;285:244-9.
[108] Amos FF, Evans JS. AP7, a Partially Disordered Pseudo C-RING Protein, Is Capable of Forming Stabilized Aragonite in Vitro†. Biochemistry 2009;48:1332-9.
[109] Huang Y-C, Chang H-H, Mou Y, Chi P, Chan JCC, Luo S-C. Purification of recombinant nacre-associated mineralization protein AP7 fused with maltose-binding protein. Protein expression and purification 2014;100:26-32.
[110] Perovic I, Verch A, Chang EP, Rao A, Cölfen H, Kröger R, Evans JS. An oligomeric C-RING nacre protein influences prenucleation events and organizes mineral nanoparticles. Biochemistry 2014;53:7259-68.
[111] Wustman BA, Morse DE, Evans JS. Structural characterization of the N-terminal mineral modification domains from the molluscan crystal-modulating biomineralization proteins, AP7 and AP24. Biopolymers 2004;74:363-76.

[112] Fu G, Valiyaveettil S, Wopenka B, Morse DE. CaCO3 biomineralization: acidic 8-kDa proteins isolated from aragonitic abalone shell nacre can specifically modify calcite crystal morphology. Biomacromolecules 2005;6:1289-98.
[113] Lopez E, Vidal B, Berland S, Camprasse S, Camprasse G, Silve C. Demonstration of the capacity of nacre to induce bone formation by human osteoblasts maintained in vitro. Tissue and Cell 1992;24:667-79.
[114] Shen X, Belcher AM, Hansma PK, Stucky GD, Morse DE. Molecular cloning and characterization of lustrin A, a matrix protein from shell and pearl nacre of Haliotis rufescens. Journal of Biological Chemistry 1997;272:32472-81.
[115] Marie B, Joubert C, Belliard C, Tayale A, Zanella-Cléon I, Marin F, Gueguen Y, Montagnani C. Characterization of MRNP34, a novel methionine-rich nacre protein from the pearl oysters. Amino acids 2012;42:2009-17.
[116] Zhang Y, Meng Q, Jiang T, Wang H, Xie L, Zhang R. A novel ferritin subunit involved in shell formation from the pearl oyster (Pinctada fucata). Comparative Biochemistry and Physiology Part B: Biochemistry and Molecular Biology 2003;135:43-54.
[117] Zhang Y, Xie L, Meng Q, Jiang T, Pu R, Chen L, Zhang R. A novel matrix protein participating in the nacre framework formation of pearl oyster, Pinctada fucata. Comparative Biochemistry and Physiology Part B: Biochemistry and Molecular Biology 2003;135:565-73.
[118] Sato Y, Inoue N, Ishikawa T, Ishibashi R, Obata M, Aoki H, Atsumi T, Komaru A. Pearl microstructure and expression of shell matrix protein genes MSI31 and MSI60 in the pearl sac epithelium of Pinctada fucata by in situ hybridization. PloS one 2013;8:e52372.
[119] Montagnani C, Marie B, Marin F, Belliard C, Riquet F, Tayalé A, Zanella-Cléon I, Fleury E, Gueguen Y, Piquemal D. Pmarg-Pearlin is a Matrix Protein Involved in Nacre Framework Formation in the Pearl Oyster Pinctada margaritifera. Chembiochem 2011;12:2033-43.
[120] Brown AH, Rodger PM, Evans JS, Walsh TR. Equilibrium conformational ensemble of the intrinsically disordered peptide n16N: linking subdomain structures and function in nacre. Biomacromolecules 2014;15:4467-79.
[121] Perovic I, Chang EP, Lui M, Rao A, Cölfen H, Evans JS. A nacre protein, n16. 3, self-assembles to form protein oligomers that dimensionally limit and organize mineral deposits. Biochemistry 2014;53:2739-48.
[122] Yan Z, Jing G, Gong N, Li C, Zhou Y, Xie L, Zhang R. N40, a novel nonacidic matrix protein from pearl oyster nacre, facilitates nucleation of aragonite in vitro. Biomacromolecules 2007;8:3597-601.
[123] Marie B, Zanella-Cléon I, Corneillat M, Becchi M, Alcaraz G, Plasseraud L, Luquet G, Marin F. Nautilin-63, a novel acidic glycoprotein from the shell nacre of Nautilus macromphalus. FEBS journal 2011;278:2117-30.
[124] Zhang C, Li S, Ma Z, Xie L, Zhang R. A novel matrix protein p10 from the nacre of pearl oyster (Pinctada fucata) and its effects on both CaCO3 crystal formation and mineralogenic cells. Marine Biotechnology 2006;8:624-33.
[125] Gong N, Shangguan J, Liu X, Yan Z, Ma Z, Xie L, Zhang R. Immunolocalization of matrix proteins in nacre lamellae and their in vivo effects on aragonitic tablet growth. Journal of structural biology 2008;164:33-40.
[126] Lao Y, Zhang X, Zhou J, Su W, Chen R, Wang Y, Zhou W, Xu Z-F. Characterization and in vitro mineralization function of a soluble protein complex P60 from the nacre of Pinctada fucata. Comparative Biochemistry and Physiology Part B: Biochemistry and Molecular Biology 2007;148:201-8.

[127] Mann K, Siedler F, Treccani L, Heinemann F, Fritz M. Perlinhibin, a cysteine-, histidine-, and arginine-rich miniprotein from abalone (Haliotis laevigata) nacre, inhibits in vitro calcium carbonate crystallization. Biophysical journal 2007;93:1246-54.
[128] Treccani L, Mann K, Heinemann F, Fritz M. Perlwapin, an abalone nacre protein with three four-disulfide core (whey acidic protein) domains, inhibits the growth of calcium carbonate crystals. Biophysical journal 2006;91:2601-8.
[129] Pan C, Fang D, Xu G, Liang J, Zhang G, Wang H, Xie L, Zhang R. A novel acidic matrix protein, PfN44, stabilizes magnesium calcite to inhibit the crystallization of aragonite. Journal of Biological Chemistry 2014;289:2776-87.
[130] Suzuki M, Saruwatari K, Kogure T, Yamamoto Y, Nishimura T, Kato T, Nagasawa H. An acidic matrix protein, Pif, is a key macromolecule for nacre formation. Science 2009;325:1388-90.
[131] Liu X, Dong S, Jin C, Bai Z, Wang G, Li J. Silkmapin of Hyriopsis cumingii, a novel silk-like shell matrix protein involved in nacre formation. Gene 2015;555:217-22.
[132] Ramos-Silva P, Benhamada S, Le Roy N, Marie B, Guichard N, Zanella-Cléon I, Plasseraud L, Corneillat M, Alcaraz G, Kaandorp J. Novel molluskan biomineralization proteins retrieved from proteomics: a case study with Upsalin. ChemBioChem 2012;13:1067-78.
[133] Marin F, Luquet G, Marie B, Medakovic D. Molluscan shell proteins: primary structure, origin, and evolution. Current topics in developmental biology 2007;80:209-76.
[134] Gao H, Chen H, Chen W, Tao F, Zheng Y, Jiang Y, Ruan H. Effect of nanometer pearl powder on calcium absorption and utilization in rats. Food chemistry 2008;109:493-8.
[135] Shao D-Z, Wang C-K, Hwang H-J, Hung C-H, Chen Y-W. Comparison of hydration, tyrosinase resistance, and antioxidant activation in three kinds of pearl powders. Journal of cosmetic science 2010;61:133.
[136] Shono M, Shimizu I, Aoyagi E, Taniguchi T, Takenaka H, Ishikawa M, Urata M, Sannomiya K, Tamaki K, Harada N. Reducing effect of feeding powdered nacre of Pinctada maxima on the visceral fat of rats. Bioscience, biotechnology, and biochemistry 2008;72:2761-3.
[137] Silve C, Lopez E, Vidal B, Smith DC, Camprasse S, Camprasse G, Couly G. Nacre initiates biomineralization by human osteoblasts maintained in vitro. Calcified Tissue International 1992;51:363-9.
[138] Atlan G, Delattre O, Berland S, LeFaou A, Nabias G, Cot D, Lopez E. Interface between bone and nacre implants in sheep. Biomaterials 1999;20:1017-22.
[139] Kim Y-W, Kim J-J, Kim YH, Rho J-Y. Effects of organic matrix proteins on the interfacial structure at the bone–biocompatible nacre interface in vitro. Biomaterials 2002;23:2089-96.
[140] Green DW, Kwon H-J, Jung H-S. Osteogenic potency of nacre on human mesenchymal stem cells. Molecules and cells 2015;38:267-72.
[141] Lamghari M, Berland S, Laurent A, Huet H, Lopez E. Bone reactions to nacre injected percutaneously into the vertebrae of sheep. Biomaterials 2001;22:555-62.
[142] Lamghari M, Huet H, Laurent A, Berland S, Lopez E. A model for evaluating injectable bone replacements in the vertebrae of sheep: radiological and histological study. Biomaterials 1999;20:2107-14.
[143] Asvanund P, Chunhabundit P, Suddhasthira T. Potential induction of bone regeneration by nacre: an in vitro study. Implant dentistry 2011;20:32-9.
[144] Bahar H, Yaffe A, Binderman I. The influence of nacre surface and its modification on bone apposition: a bone development model in rats. Journal of periodontology 2003;74:366-71.

[145] Fricain JC, Cognet J, Réau A, Lavignolle B. In Vivo Study of Nacre Pinctada Margaritifera Behaviour in Subcutaneous Site in Rat. Key Engineering Materials: Trans Tech Publ; 2005. p. 965-70.
[146] Duplat D, Chabadel A, Gallet M, Berland S, Bédouet L, Rousseau M, Kamel S, Milet C, Jurdic P, Brazier M. The in vitro osteoclastic degradation of nacre. Biomaterials 2007;28:2155-62.
[147] Berland S, Delattre O, Borzeix S, Catonné Y, Lopez E. Nacre/bone interface changes in durable nacre endosseous implants in sheep. Biomaterials 2005;26:2767-73.
[148] Liao H, Mutvei H, Hammarström L, Wurtz T, Li J. Tissue responses to nacreous implants in rat femur: an in situ hybridization and histochemical study. Biomaterials 2002;23:2693-701.
[149] Li X, Pan D, Lin S, Zhuang Z, Lin Z. Facile in vitro hydroxyapatite remineralization of human enamel with remarkable hardness. CrystEngComm 2013;15:4351-6.
[150] Miyoshi T, Matsuda Y, Komatsu H. Fluorescence from pearls to distinguish mother oysters used in pearl culture. Jpn J Appl Phys 1987;26:578-81.
[151] Oaki Y, Imai H. The hierarchical architecture of nacre and its mimetic material. Angewandte Chemie International Edition 2005;44:6571-5.
[152] Liao H, Mutvei H, Sjöström M, Hammarström L, Li J. Tissue responses to natural aragonite (Margaritifera shell) implants in vivo. Biomaterials 2000;21:457-68.
[153] Lamghari M, Antonietti P, Berland S, Laurent A, Lopez E. Arthrodesis of lumbar spine transverse processes using nacre in rabbit. Journal of Bone and Mineral Research 2001;16:2232-7.
[154] Rousseau M, Delattre O, Gillet P, Lopez E. Subchondral nacre implant in the articular zone of the sheep's knee: A pilot study. Bio-medical materials and engineering 2012;22:227-34.
[155] Liu Y, Huang Q, Feng Q, Hu N, Albert O. Structural features and mechanical properties of PLLA/pearl powder scaffolds. Journal of Mechanics in Medicine and Biology 2013;13:1350020.
[156] Liu Y, Huang Q, Feng Q. 3D scaffold of PLLA/pearl and PLLA/nacre powder for bone regeneration. Biomedical Materials 2013;8:065001.
[157] Liu Y, Huang Q, Kienzle A, Müller W, Feng Q. In vitro degradation of porous PLLA/pearl powder composite scaffolds. Materials Science and Engineering: C 2014;38:227-34.
[158] Dai J, Bai J, Jin J, Yang S, Li G. Stimulation by Pearl of Mineralization and Biocompatibility of PLA. Advanced Engineering Materials 2015;17:1691-7.
[159] Xiao W-D, Zhong Z-M, Tang Y-Z, Xu Z-X, Xu Z, Chen J-T. Repair of critical size bone defects with porous poly (D, L-lactide)/nacre nanocomposite hollow scaffold. Saudi medical journal 2012;33:601-7.
[160] Yang Y-L, Chang C-H, Huang C-C, Kao WM-W, Liu W-C, Liu H-W. Osteogenic activity of nanonized pearl powder/poly (lactide-co-glycolide) composite scaffolds for bone tissue engineering. Bio-medical materials and engineering 2014;24:979-85.
[161] Xu M, Li Y, Suo H, Yan Y, Liu L, Wang Q, Ge Y, Xu Y. Fabricating a pearl/PLGA composite scaffold by the low-temperature deposition manufacturing technique for bone tissue engineering. Biofabrication 2010;2:025002.
[162] Liu Y, Sinha SK. Wear performances and wear mechanism study of bulk UHMWPE composites with nacre and CNT fillers and PFPE overcoat. Wear 2013;300:44-54.
[163] Meifeng H, Xianyang H, Xue F, Deng P. In vitro corrosion behavior and biocompatibility of biodegradable magnesium-pearl powder metal matrix composite. Journal of Alloys and Compounds 2016;663:156-65.

[164] Tao L, Zhu J, Shen Y, Ruan H. The Composite Material of Pearl Powder/PEEK quasi natural bone, its preparation method and applications. CN 100427150C. China. 2008.
[165] Meng XH GL. In Vitro Mineralization of Poly(3-hydroxybutyrate-co-3-hydroxyvalerate) Blended with Pearl Powders by Incubation in Simulated Body Fluids. International Forum on Biomedical Textile Materials, Proceedings 2010;124.
[166] Bai J, Dai J, Li G. Electrospun composites of PHBV/pearl powder for bone repairing. Progress in Natural Science: Materials International 2015;25:327-33.
[167] Deng Y, Li G, Song W, Jiang J. Preparation and properties of pearl powder/polypropylene composites and their biocompatibility. Bio-Medical Materials and Engineering 2015;26:S27-S34.
[168] Li-Qin Z, Hui-Ming W, Jun-Hua X, Dong W, Wen-Quan Z, Xiao-Xiang W, Nan-Ping W. Effects of titanium implant surface coated with natural nacre on MC3T3E1 cell line in vitro. Progress in Biochemistry and Biophysics 2008;35:671-5.
[169] Zhu L, Wang H, Xu J, Lin J, Wang X. Effects of nacre-coated titanium surfaces on cell proliferation and osteocalcin expression in MG-63 osteoblast-like cells. African Journal of Biotechnology 2011;10:15387-93.
[170] Guo Y, Zhou Y. Transformation of nacre coatings into apatite coatings in phosphate buffer solution at low temperature. Journal of Biomedical Materials Research Part A 2008;86:510-21.
[171] Kwan M, Wang RZ. Bio-Fabrication of Nacre on Conventional Implant Materials. Key Engineering Materials: Trans Tech Publ; 2013. p. 255-60.
[172] Wang XX, Xie L, Luo C, Wang RZ. Natural Nacre Coatings on Titanium Implant Grown by Fresh Water Bivalve Shell. Key Engineering Materials: Trans Tech Publ; 2006. p. 743-6.
[173] Wang X-X, Xie L, Wang R. Biological fabrication of nacreous coating on titanium dental implant. Biomaterials 2005;26:6229-32.
[174] Brion A, Zhang G, Dossot M, Moby V, Dumas D, Hupont S, Piet M, Bianchi A, Mainard D, Galois L. Nacre extract restores the mineralization capacity of subchondral osteoarthritis osteoblasts. Journal of structural biology 2015;192:500-9.

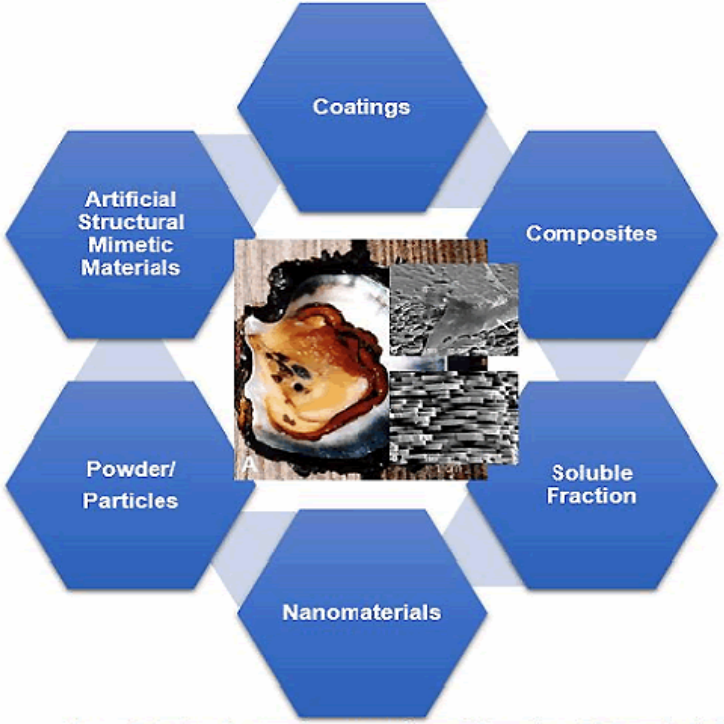

Mussel derived nacre is a novel, multifunctional biomaterial